Characterization of Electrochemically Co-deposited Metal−Molybdenum Oxide Films

A. C. Pereira,[†] T. L. Ferreira,[†] L. Kosminsky,[†] R. C. Matos,[‡] M. Bertotti,[†] M. H. Tabacniks,[§] P. K. Kiyohara,[§] and M. C. A. Fantini*[,§]

Instituto de Química, USP, CP 26077, CEP 05599-970, São Paulo, SP Brazil, Departamento de Química, UFJF, CEP 36038-330, Juiz de Fora, MG Brazil, and Instituto de Física, USP, CP 66318, CEP 05315-970, São Paulo, SP Brazil

Received February 4, 2004

Molybdenum oxide films with and without metal inclusions were electrochemically deposited on glassy carbon electrodes and characterized by soft X-ray spectroscopy, X-ray diffraction, scanning electron microscopy, and Rutherford backscattering spectroscopy. The local coordination of Mo is preferentially octahedral, but changes in the composition promote the appearance of tetrahedral Mo sites. The Mo local structure configurations were evaluated when different potential cycles were used in the modification of the electrode surface. Some metals (Pt, Pd, Rh, and Cu) were co-deposited with the Mo species and their effect on the obtained material was investigated. Pt and Cu favored the formation of bronzes and the enrichment of the film with tetrahedral units of MoO_x. The occupancy level of the 4d orbital of Mo was examined as an indicator of interactions between Mo and co-deposited metals.

Introduction

Aqueous species of Mo(VI) present a complex chemistry as a consequence of various protonation and polymerization equilibria, depending on the experimental conditions, like pH and concentration.[1,2] The deposition of molybdenum species on solid surfaces by adsorption from solutions,[3,4] chemical vapor deposition (CVD),[5] sol−gel,[6,7] or electrochemical techniques[8] produces nonstoichiometric oxides (named as MoO_{3-x}) or bronzes (H_x-MoO_3). The intercalation of protons or alkaline metallic ions in the interstices of these oxides occurs as a consequence of charge compensation,[9] generating structural changes[10] and electrochromic effects.[11−13]

In our previous works, chemical and electrochemical properties of immobilized molybdenum oxides were investigated, especially due to the capacity of these oxides to act as catalyst or mediator in some reactions. The activity of these surfaces toward reductive processes is dependent on structural disorder near the metallic centers, where changes of the Mo oxidation state take place by the intercalation of hydrogen atoms, generating bronzes by the spillover effect.[14] Accordingly, we have shown that the cathodic reduction of both bromate[8] and iodate[15] is facilitated at glassy carbon surfaces coated with molybdenum oxide layers. On the other hand, anodic processes involving the MoO_3 film have also been investigated, such as in the case of (NO_2^-)[16] and NO[17] electrochemical oxidation. The current enhancement associated with these anodic processes was attributed to the facilitation of electronic transfer toward metallic sites[18] or by a mechanism based on a fast O-atom transfer.[19,20] We have also shown that a film with a better performance for hydrogen peroxide oxidation is obtained by co-deposition of platinum microparticles and molybdenum oxides,[21] comparative studies being performed with platinized gold electrodes.

Compositional changes are correlated with the electrochemical behavior when Mo oxides act as a catalyst or mediator. For instance, by conjugating many techniques, Mestl et al.[22] investigated the influence of both structure and composition of Mo oxides on the catalytic

* Corresponding author. Phone: +55-11-3091-6882. Fax: +55-11-3091-6749. E-mail: mfantini@if.usp.br.
[†] Instituto de Química, USP.
[‡] Departamento de Química, UFJF.
[§] Instituto de Física, USP.

(1) Tytko, K. H.; Baethe, G.; Cruywagen, J. J. *Inorg. Chem.* **1985**, *24*, 3132.
(2) Cruywagen, J. J.; Draaijer, A. G. *Polyhedron* **1992**, *11*, 141.
(3) Cruywagen, J. J.; De Wet, H. F. *Polyhedron* **1998**, *7*, 547.
(4) Ioroi, T.; Fujiwara, N.; Siroma, Z.; Yasuda, K.; Miyazaki, Y. *Electrochem. Commun.* **2002**, *4*, 442.
(5) Ivanova, T.; Surtchev, M.; Gesheva, K. *Mater. Lett.* **2002**, *53*, 250.
(6) Dong, W.; Dunn, B. *J. Mater. Chem.* **1998**, *8* (3), 665.
(7) Dong, W.; Dunn, B. *J. Non-Cryst. Solids* **1998**, *225* (1), 135.
(8) Bertotti, M.; Pletcher, D. *Electroanalysis* **1996**, *8*, 1105.
(9) Wang, B.; Dong, S. *J. Electroanal. Chem.* **1994**, *379*, 207.
(10) Ferreira, F. F.; Cruz, T. G. S.; Fantini, M. C. A.; Tabacniks, M. H.; de Castro, S. C.; Morais, J.; de Siervo, A.; Landers, R.; Gorenstein, A. *Solid State Ionics* **2000**, *136−137*, 357.
(11) Lee, S-H.; Seong, M. J.; Tracy, C. E.; Mascarenhas, A.; Pitts, J. R.; Deb, S. K. *Solid State Ionics* **2002**, *147*, 129.
(12) Watson, R. B.; Ozkan, U. S. *J. Phys. Chem. B* **2002**, *106*, 6930.
(13) Guay, D.; Tourillon, G.; Laperriere, G.; Bélanger, D. *J. Phys. Chem.* **1992**, *96*, 7718.
(14) Xie, Y. C.; Wang, X. Y.; Tang, Y. Q. *Stud. Surf. Sci. Catal.* **1997**, *112*, 49.
(15) Kosminsky, L.; Bertotti, M. *Electroanalysis* **1999**, *11* (9), 623.
(16) Kosminsky, L.; da Paixão, T. R. L. C.; da Rocha, J. R. C.; Bertotti, M. *Electroanalysis* **2001**, *13* (2), 155.
(17) Kosminsky, L.; Mori, V.; Bertotti, M. *J. Electroanal. Chem.* **2001**, *499*, 176.
(18) Zhang, H. Q.; Wang, Y.; Fachini, E. R.; Cabrera, C. R. *Electrochem. Solid State* **1999**, *2* (9), 437.
(19) Kawagoe, K. T.; Johnson, D. C. *J. Electrochem. Soc.* **1994**, *141*, 3414.
(20) Feng, J.; Johnson, D. C. *J. Electrochem. Soc.* **1990**, *137*, 507.
(21) Kosminsky, L.; Matos, R. C.; Tabacniks, M. H.; Bertotti, M. *Electroanalysis* **2003**, *15*, 733.

10.1021/cm040125t CCC: $27.50
Published on Web 06/02/2004

activity. They also demonstrated that the induced oxygen deficiencies in the bulk of molybdenum oxides, changing from MoO_3 to MoO_2, can be followed by thermal techniques. Oxides, composed of well-characterized Mo (IV, V, and VI) species, presented different behaviors in redox or electronic transfer processes.[22]

Compounds with Mo in these oxidation states were chemically prepared by controlling the implantation flux of oxygen ions and the amount of oxygen incorporation in a substrate of metallic molybdenum. Also, by controlling some parameters of formation, Renner et al.[23] detected, by X-ray diffraction (XRD), a molybdenum oxide δ-MoO_2 phase, before covering the surface by an amorphous oxide layer, differently from Al-Kuhaili et al.,[24] who obtained only amorphous phases with changes in the thickness of the film.

The oxide has the ability to promote a direct interaction with some substrates, as oxyanions, since they allow oxygen transfer to occur between substrate and oxide simultaneously to the electron transfer. Catalysis is enhanced by the co-deposition of other metal oxides, as vanadium, tungsten, and niobium,[25,26] or metallic center such as Pt.[4,21] Ioroi et al.[4] reported that insertion of platinum was responsible for the decrease of the crystallinity of the deposited oxides and for the change in lattice parameters.

Fielicke and Rademann[27] studied molybdenum-doped bismuth oxide clusters as the catalyst for ethene reactions. They observed that the reactivity of the highly active bismuth oxide clusters ($Bi_6O_9^+$) is only slightly varied by the addition of one MoO_3 unit, thus providing evidence for the independence of the different metal oxide centers in the cluster.[27] Changes observed in the catalytic power of Mo−MnO after calcination, which generate an oxygen vacancy in the lattice, producing Mo(V) species,[28] are attributed only to the surface architecture.

Also, the local structure of the immobilized material depends on the composition, structure, and morphology of the support. By working with different substrates such as SiO_2 and TiO_2 as matrixes for the deposition of molybdenum oxides, Radhakrishnan et al.[29] reported different coordination symmetries for molybdenum oxides, as isolated tetrahedrons and a mixture of tetrahedrons and distorted octahedrons. The ordered formation of molybdenum oxide nanoparticles on oriented surfaces is also a starting point for studying the effects of O vacancies in films presenting different behaviors and chemical properties.[30]

XANES is an excellent technique for local symmetry characterization of nanodispersed molybdenum oxide phases. The Mo $L_{2,3}$ edges (2.52 keV for the L_3 edge and 2.63 keV for the L_2 edge) are very pronounced and may supply information about the oxidation state and coordination of molybdenum sites.[29,31] Absorption spectra of MoO_x present two peaks at the L_3 edge, and the distance of each other is correlated to the Mo coordination.[29,32] Accordingly, Mo atoms in the +6 state display d-orbital splitting in the 1.8−2.4 eV range for tetrahedral Mo site geometry, whereas octahedral-coordinated molybdates display splitting in the 3.1−4.5 eV range.[31] The edge position is an indicative parameter of the oxidation state of the analyzed sample. Larger edge energy values are associated with more oxidized species, as demonstrated in studies involving measurements of the K edge.[33]

The most employed growth technique of thin films of molybdenum oxides is CVD. However, this procedure requires thermal treatment and elevated pressure. At these experimental conditions, physical properties of the films are significantly altered and a decrease in their resistivity is also observed,[32] generally transforming all the deposited material to the most oxidized species. On the other hand, electrochemical procedures are advantageous, as they are simple and allow fine control of the film thickness. Besides this, metal co-deposition may be carried out as a continuous process, permitting a uniform distribution in the bulk of the film. Presently, there is no report on a systematic study involving electrochemically deposited films of molybdenum oxides with respect to their surface characterization in the presence of metallic particles. Accordingly, in this work we report results on the use of soft X-ray spectroscopy (XAS) and Rutherford backscaterring spectroscopy (RBS) techniques to investigate the structure and composition of MoO_x films, electrochemically deposited at different experimental conditions. Scanning electron microscopy (SEM) and XRD were utilized to complete the material's characterization.

Experimental Section

Reagents. All reagents used were of analytical grade and were used as received. Solutions were prepared by dissolving the solids in distilled water that was also treated with a Nanopure Infinity water purification system. Molybdate stock solutions (10 mmol·L^{-1}) were prepared from the sodium salt. Pt(II), Pd(II), and Rh(III) stock solutions (100 mmol·L^{-1}) were prepared from the chloride salts, dissolved in HCl (100 mmol·L^{-1}). Solutions were bubbled with argon for 5 min prior to each electrode surface modification procedure.

Modification of the Electrode Surface. The electrodeposition of a layer of molybdenum oxide onto the electrode surface was carried out by cycling consecutively the potential of the working carbon electrode (polished previously with alumina powder, 1 μm, and further rinsing with deionized water) in a solution containing 1 mmol·L^{-1} Mo(VI) in 50 mmol·L^{-1} Na_2SO_4 (at pH 3.0) from +0.2 to −0.8 V. When not specified, 10 potential cycles were employed for the modification procedure. After the film deposition, the electrode was rinsed with deionized water to remove traces from the Mo(VI) solution.

(22) Mestl, G.; Linsmeier, Ch.; Gottschall, R.; Dieterle, M.; Find, J.; Herein, D.; Jäger, J.; Uchida, Y.; Schlögl, R. *J. Mol. Catal. A: Chem.* **2000**, *162*, 463.
(23) Renner, B.; Hammerl, C.; Rauschenbach, B. *Nucl. Instrum. Methods Phys. Res., Sect. B* **2000**, *160*, 363.
(24) Al-Kuhaili, M. F.; Durrani, S. M. A.; Khawaja, E. E. *Thin Solid Films* **2002**, *418*, 188.
(25) Ovsitser, O.; Uchida, Y.; Mestl, G.; Weinberg, G.; Blume, A.; Jäger, J.; Dieterle, M.; Hibst, H.; Schlögl, R. *J. Mol. Catal. A: Chem.* **2002**, *185*, 291.
(26) Chary, K. V. R.; Kumar, C. P.; Reddy, K. R.; Bhaskar, T.; Rajiah, T. *Catal. Commun.* **2002**, *3*, 7.
(27) Fielicke, A.; Rademann, K. *Chem. Phys. Lett.* **2002**, *359*, 360.
(28) Cadus, L. E.; Ferretti, O. *Appl. Catal., A* **2002**, *233*, 239.
(29) Radhakrishnan, R.; Reed, C.; Oyama, S. T.; Seman, M.; Kondo, J. N.; Domen, K.; Ohminami, Y.; Asakura, K. *J. Phys. Chem. B* **2001**, *105*, 8519.
(30) Chang, Z.; Song, Z.; Liu, G.; Rodriguez, J. A.; Hrbek, J. *Surf. Sci.* **2002**, *512*, L353.
(31) Bare, S. R.; Mitchell, G. E.; Maj, J. J.; Vrieland, G. E.; Gland, J. L. *J. Phys. Chem.* **1993**, *97*, 6048.
(32) Miyata, N.; Suzuki, T.; Ohyama, R. *Thin Solid Films* **1996**, *282* (1−2), 218.
(33) Ressler, T.; Wienold, J.; Jentoft, R. E.; Neisius, T. *J. Catal.* **2002**, *210*, 67.

For co-deposition of metallic ions, solutions containing the corresponding cations were added to the working Mo(VI) solution.

Apparatus. Potentials were applied by using an EG&G 273A potentiostat connected to a 486 DX computer. The electrochemical cell was of standard design and consisted of a glassy carbon electrode (1 cm^2), a Pt auxiliary electrode, and a Ag | AgCl | $NaCl_{(sat)}$ reference electrode.

The X-ray diffraction (XRD) $\theta-2\theta$ measurements ($10° < 2\theta < 55°$) were performed using Ni-filtered Cu Kα radiation (1.2 kW). The diffractograms were taken by step scanning mode, with steps of 0.05°. The counting time was 10 s. Rutherford backscattering spectrometry (RBS) analysis was done using a 2.385 MeV He^+ beam with a scattering angle of 170° at the LAMFI, Instituto de Física, USP, São Paulo, Brazil, using a 5SDH NEC Pelletron-tandem accelerator.[34] RBS spectra were analyzed and simulated using RUMP.[35] Hydrogen concentrations were measured by the deficit method, hence its high uncertainty. Oxygen concentrations were corrected by a factor of 1.14 ± 0.02 to compensate for the non-Rutherford cross section at 2.4 MeV. Film thicknesses were calculated by converting the measured atomic densities (atoms·cm^{-2}) using tabulated mass densities except for H (0.07 g·cm^{-3}) and O (1.14 g·cm^{-3}). The scanning electron microscopy (SEM) pictures, taken before and after sample's washing in water, with and without ultrasound, were obtained with a JEOL microscope, model JSM 841, equipped with an X-ray spectrometer (EDS), operating at 25 kV. The modified electrodes, composed of ultradense amorphous carbon substrate, present enough electric conductivity to perform the SEM analysis with no need of metallic covering. Therefore, the samples were directly glued onto the microscope sample holder.

X-ray absorption spectroscopy measurements at the Mo L edge (≈2.5 keV), the Rh L edge (≈3.0 keV), the Pd L edge (≈3.15 keV), and the Pt M edge (≈2.65 keV), were recorded at the National Syncrotron Light Source (LNLS), Campinas, São Paulo, Brazil, at the SXS beamline. The Cu L edge (≈0.93 keV) was not measured due to technical problems. The monochromator was an InSb (111) double crystal with a constant beam height. The energy resolution of the line was $\Delta E = 0.2$ eV. The focusing element was a toroidal mirror (Zerodur with gold layer). The detection was done by the total current (TEY) mode, measured over the sample with an electrometer. The mean free path of the detected electrons is estimated to be of the order of the film's thickness, ~30 nm; therefore, the X-ray absorption spectroscopy measurements represent the whole film volume.[36,37]

Results and Discussion

The solution chemistry of Mo(VI) is very rich and dominated by polymerization reactions, which leads to the formation of monomers, dimers, and more condensed Mo(VI) species.[2,3] Consequently, the electrochemistry of Mo(VI) solutions has been shown to be very complicated and dependent on the nature of the electrode material because adsorption processes are rate-determining in some specific conditions.[38] At relatively dilute Mo(VI) solutions (i.e., $C_{Mo(VI)} < 1$ mM), monomers and dimers prevail in solution and electrochemistry shows reductive processes at glassy carbon surfaces at a pH range comprising 2 and 6. The magnitude of both cathodic and anodic processes changes with the pH, higher signals being obtained at pH values around 3.0. At this experimental condition, a black layer covers the electrode surface upon continuous potential cycling, indicating that the material formed during the reductive potential sweep is insoluble and is deposited on the electrode surface as an oxide film.

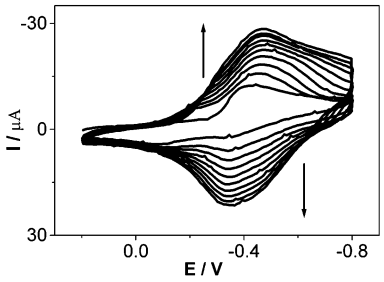

Figure 1. Voltammetric cycles of the electrochemical deposition of molybdenum oxides by cycling consecutively the potential in solutions containing Mo(VI).[15]

Figure 1 shows a typical experiment involving the electrochemical deposition of molybdenum oxides by cycling consecutively the potential in solutions containing Mo(VI). Voltammograms obtained after the first two potential cycles exhibited a cathodic wave (peak potential at around −0.50 V) and two anodic waves (at −0.35 and −0.10 V). The shape of the resulting voltammogram is dependent on experimental conditions, that is, Mo(VI) concentration and acidity, as different species may exist in solution. Also, during consecutive potential cycles a film composed of insoluble molybdenum oxide is deposited on the electrode surface and the equilibrium among various oxides in different phases causes the voltammetric profile to change depending on the amount of material covering the electrode surface.[15] The voltammetric behavior of the modified electrode in a free-Mo(VI) supporting electrolyte solution is identical to the final voltammogram obtained during the modification procedure, demonstrating that the electrogenerated film is adherent to the electrode surface.

The surface's morphology and atomic composition of the electrodeposited molybdenum oxide films was examined by SEM, coupled with EDS. Figure 2a shows the morphology of the co-deposited material obtained from repetitive potential cycling in a solution containing 1 mM Mo(VI) plus 0.01 mM Pt(II), after superficial washing in water. As can be seen from this image, the film presents a cauliflower type of morphology, typical of electrodeposited compounds.[39] Because of the differences in mechanical properties of the film and substrate, drying the sample induces cracks on the surface. No bright spots, which would indicate the existence of metallic microparticles, are visible in this picture.[40] Also, the EDS analysis did not show any peak that could be attributed to Pt, demonstrating that the Pt content is very small (likely less than 1 at. % in total), probably indicating that Pt is atomically dispersed in the oxide matrix. Moreover, the XRD data did not show any trace of crystalline Pt; neither its absorption edge could be visualized during the X-ray absorption measurements in samples deposited with 1 mM Mo(VI) plus 0.01 mM

(34) Tabacniks, M. H. The Laboratory for Material Analysis with Ion Beams. LAMFI − USP. In *Nuclear Physics*; Souza, S. R., Gonçalves, O. D., Lima, C. L., Tomio, L., Vanin, V. R., Eds.; World Scientific: Singapore, 1998.
(35) Doolittle, L. R. *Nucl. Instrum. Methods* **1985**, *B9*, 344.
(36) Okude, N.; Noro, H.; Nagoshi, M.; Yamamoto, H.; Baba, Y.; Sasaki, J. *J. Electron Spectrosc.* **1998** *88*, 467.
(37) Noro H, H.; Nagoshi, M. *Tetsu to Hagane* **2003**, *89*, 109.
(38) Lowinsohn, D.; Bertotti, M. *Electroanalysis* **2002**, *14*, 619.
(39) Schrebler, R.; Merino, M.; Cury, P.; Romo, M.; Cordova, R.; Gomez, H.; Dalchiele, E. A. *Thin Solid Films* **2001**, *388*, 201.
(40) Ferreira, F. F.; Haddad, P. S.; Fantini, M. C. A.; Brito, G. E. S. *Solid State Ionics* **2003**, *165*, 161.

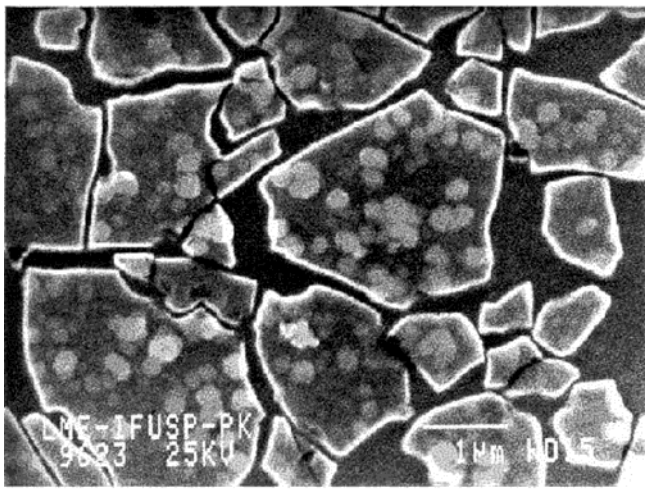

(a)

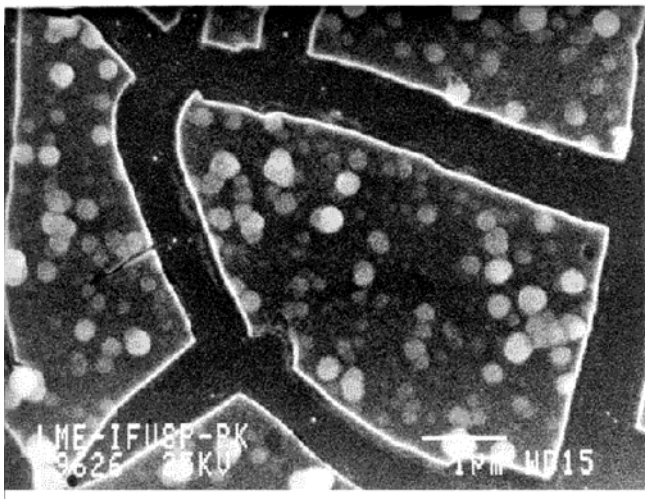

(b)

Figure 2. (a) SEM picture of a film prepared with 1 mM Mo and (b) SEM picture of a film prepared with 1 mM Mo plus 0.01 mM Pt, both deposited with 10 cycles.

Pt(II). To check if the observed lumps on top of the films are really part of it or untied particles, the samples were washed under ultrasound agitation. The film's morphology remained unchanged, as can be observed in Figure 2b, showing that the surface of the deposited film indeed presents high roughness; in this case, also, no trace of Pt was detected in the EDS spectra.

Film thickness is easily controlled by measuring the number of potential cycles involved in the modification procedure, as demonstrated by RBS measurements shown in Table 1.

Table 1 shows that relatively thin films (three potential cycles) present the higher O/Mo ratio; that is, the oxidation state of molybdenum is more elevated. Values of O/Mo ratio may suffer strong deviation from the theoretical ones, as observed by Mestl et al.[22] in XPS experiments, but they can be comparatively evaluated. Films produced with 10 potential cycles show higher amounts of hydrogen as a consequence of the formation of bronzes. This is in agreement with previous studies on the higher efficiency of molybdenum oxide films prepared with 10 potential cycles on the electrocatalysis of iodate reduction,[15] once bronzes are better catalysts than oxides.[41] Similar results were obtained by Matsuda et al.[41] for the activity of isomerization of pentane. They observed that the presence of a phase composed by bronzes of molybdenum, in the heated molybdenum oxides physically mixed with Pt, increased the area of the material and modified the chemical nature of the surface. The rate activity of isomerization of pentane was enhanced due to the occurrence of interactions between the pentane and the bronzes, which confer higher extension of the reaction of isomerization and generates active sites related to the formation of the MoO_xH_y phase, derived from a H_xMoO_3 phase.[41]

Table 1. Relative Concentrations to Molybdenum of RBS Analysis for Composition and Thickness of Mo Films Obtained with a Different Number of Potential Cycles for the Deposition of Mo Species, and with 10 Cycles for the Co-deposition of Metals and Mo Species

modifier solution composition (mol/L)	thickness (nm ± 5%)	H/Mo (±20%)	Pt/Mo (±5%)	Cu/Mo (±5%)	(O-4·S)/Mo (±7%)
Mo(VI) 10^{-3} (3 cycles)	4	0.0			4.1
Mo(VI) 10^{-3} (10 cycles)	33	4.0			2.8
Mo(VI) 10^{-3} (30 cycles)	41	0.0			2.5
Mo(VI) 10^{-3} (60 cycles)	110	1.0			2.7
Mo(VI) 10^{-3} and Cu(II) 10^{-5}	35	2.0		0.04	2.7
Mo(VI) 10^{-3} and Cu(II) 6×10^{-4}	60	5.5		1.0	3.9
Mo(VI) 10^{-3} and Cu(II) 10^{-3}	45	6.0		2.2	4.9
Mo(VI) 10^{-3} and Pt(II) 10^{-5}	60	7.5	0.10		2.6

Table 1 also shows that the amount of Cu electrodeposited is directly proportional to the Cu(II) concentration in the modifier solution; hence, it seems that molybdenum oxide does not influence Cu deposition. However, films obtained from a solution containing 6×10^{-4} mol·L^{-1} Cu(II) are thicker than those grown from more concentrated solutions containing Cu(II) (1×10^{-3} mol·L^{-1}). Moreover, films obtained from solutions with the same amount of Mo(VI) and Cu(II) present more Cu than Mo, suggesting that Cu is deposited preferentially in comparison with molybdenum oxide. This indicates that the deposited material from solutions with relatively high Cu(II) concentration in comparison to Mo(VI) consists of a metallic Cu film with some molybdenum oxide fragments on the surface, instead of a porous film of molybdenum oxide with intercalated copper particles. The loss of porosity may decrease the interlamellar distance and, consequently, may decrease the thickness of the film.

The ratio O/Mo in the deposit increases with increasing the amount of deposited Cu. This may be attributed to the formation of Cu oxides in the interstices of molybdenum oxides. The same relationship was observed for the H/Mo ratio, indicating that the presence of co-deposited Cu species facilitates the formation of bronzes.

The data in Table 1 also show that Pt was preferentially deposited in comparison to molybdenum, even being present in the working solution at significant lower levels. For instance, the Mo/Pt in the generated film was 10/1, although this relationship in the working

(41) Matsuda, T.; Hanai, A.; Uchijima, F.; Sakagami, H.; Takahashi, N.; *Microporous Mesoporous Mater.* **2002**, *51*, 155.

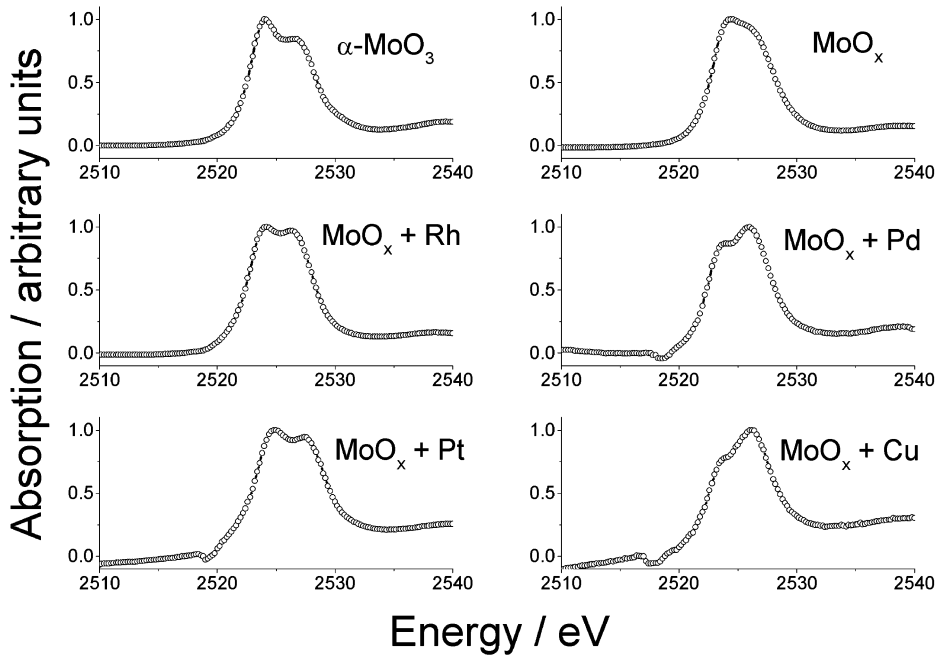

Figure 3. L_3 absorption edge for the standard α-MoO_3 and of modified electrodes by Mo oxides or bronzes with and without Pt, Pd, Rh, and Cu co-deposition, from solution containing 1 mmol·L^{-1} Mo(VI) and 1 mmol·L^{-1} metal cations.

solution was 100/1 (considering Mo(VI) and Pt(II)). For films containing platinum particles, the O/Mo ratio is significantly decreased in comparison with films prepared in the absence of platinum and this is in agreement with the concurrent increase in the H/Mo ratio as a consequence of the spillover effect.

The absolute amount of Mo atoms changed from 18.6 $\times$ 10^{15} atoms·cm^{-2}, in the absence of Pt, to 48.1 $\times$ 10^{15} atoms·cm^{-2}, in the presence of Pt. This observation is in agreement with the increase of the film thickness, as shown in Table 1. Pt co-deposition affects to a larger extent the thickness and the composition of Mo oxides than Cu in a similar process owing to the efficiency of H^+ discharge at platinum surfaces, inducing the formation of bronzes.

The starting point for the structure analysis of the films was a preliminary study employing XRD. Molybdenum oxide films were electrochemically deposited on glassy carbon and gold electrodes in the absence and in the presence of metals such as Pt, Pd, Rh, and Cu. The obtained diffractograms indicated that all analyzed films were amorphous. These results indicate that the material is not ordered if prepared according to the proposed electrochemical procedure. As a matter of fact, Mestl et al.[22] reported that Mo_5O_{14} subunits appear in mixed oxides. Different is the material immobilized by the deposition−precipitation method that presents structural regularities, loosing their crystallinity only by Pt insertion.[4]

It is important to mention that both RBS and XAS are high-vacuum techniques, which may lead to desorption of only interstitial water. The water plays an important role in the composition and structure of the Mo-oxides films,[42] maintaining their porous structure. However, the Mo−O bond is not broken by the vacuum at which RBS and XAS experiments were performed since the bond dissociation energy, 5.44 eV,[43] is very high. Furthermore, the formation of the electrodeposited material involves the cathodic reduction of Mo(VI) ions at the electrode surface in a process from which electrons are delivered to the electroactive species. To maintain the charge balance, protons penetrate through the channels of the film; the equation shown below represents the overall electrochemical process at the cathode:

$$MoO_3 + xH^+ + xe^- \rightleftharpoons H_xMoO_3$$

This equation clearly shows that molecular oxygen is not involved in the formation of the film. Hence, the reduction of the amount of oxygen in contact with the oxide film is not expected to lead to changes in the oxidation state of the metallic ion; that is, the reduction of Mo(VI) is dependent only on the heterogeneous electron-transfer process.

The structural characterization of the electrodeposited Mo oxides was performed, using the standard α-MoO_3 compound as reference. Figure 3 shows the L_3 absorption edge of the standard α-MoO_3 and of films deposited by the electrochemical method in the absence and presence of metallic particles. Different behaviors were noticed with respect to the relative intensities of the two peaks, qualitatively indicating that the metal co-deposition affects the nearest molybdenum neighborhood. This influence is more pronounced for films containing Pd and Cu since for both spectra the second peak (higher energy) exhibits larger absorption in comparison to the first one.

No changes in the oxidation state of Mo in films containing metallic particles were noticed by the absorption edge analysis since energy values did not vary significantly from the value obtained for the standard

(42) Vink, T. J.; Verbeek, R. G. F. A.; Snijders, J. H. M.; Tamminga, Y. *J. Appl. Phys.* **2000**, *87* (10), 7252.

(43) Broclawik, E.; Piskorz, W.; Adamska, K. *J. Phys. Chem.* **1999**, *110*, 11685.

α-MoO_3 (2523.0 eV). In a review about X-ray spectroscopy techniques, Chen reports that the measurement of the edge displacement is not sensible enough to characterize changes in the oxidation state of Mo species.[44] Alternatively, analysis of the L_3/L_2 ratio would serve as a qualitative indication of the oxidation state change since this ratio decreases with increasing the oxidation state of the element. Accordingly, measurements of the L_3/L_2 ratio were performed for the samples deposited with (and without) 1% of metal particles in the solution. The values were found as 1.64 ± 0.10 for the standard α-MoO_3 and 1.98 ± 0.10 for the film without metal, MoO_x. This result shows that the single film contains Mo in an oxidation state lower than +6. For molybdenum oxide films containing the metals, the L_3/L_2 ratio values were 2.11 ± 0.10 for Pt, 1.91 ± 0.10 for Pd, and 1.80 ± 0.10 for Rh. Therefore, all of them contain reduced Mo species. Also, the data are in agreement with RBS results, which indicated that molybdenum in films containing co-deposited Pt presents the lowest oxidation state. The films containing Pd and Rh are also composed by reduced molybdenum species, but to an extent similar to that of the single film. Other authors observed an increase of the catalytic effect of these (Pd, Rh)-composite materials.[45,46] On the other hand, the lower value for oxides containing Cu ($L_3/L_2 = 1.65 \pm 0.10$) indicates that the Mo became more oxidized when copper is added to the film. We may speculate that an electron sharing between Mo and Cu may be responsible for such a different value leading to an increase in the conductivity of the material.

According to Chen,[44] the lower the area obtained by integrating the L_3 edge (fitted using two Gaussian peaks), the more occupied are the Mo 4d orbitals. On the other hand, an increase in this area provoked by the co-deposited metal indicates that it does not change the Mo bondings.

The calculated area under the L_3 edge for the electrodes modified in a solution containing the same concentration of Mo(VI) and metal cations were all lower than the calculated ones for the modified electrode without metal co-deposition. This means a larger electron population of the Mo 4d orbital in the presence of co-depositing metals, enhancing the reactivity of the Mo film.[47] Co-deposited materials containing relatively high amounts of metals may also generate large nucleation of metallic sites, without interfering in the formation of the Mo sites. The area under the L_3 edge decreases significantly by co-depositing Cu, probably because of interactions between Mo and Cu by oxygen bonds. For electrodes modified in solutions with 10−100 times relative excess of Mo(VI) to the metallic ions, the areas under the L_3 edge are larger than those obtained without metal co-deposition. This is an indication that there is no direct interaction or oxygen bond between the Mo and the co-deposited metallic atom. This suggests that our previous observations on the catalytic effect of mixed electrodes containing low amounts of Pt in relation to molybdenum oxide[21] is more due to changes in both the structure and the Mo electronic distribution than by direct interactions between Mo and the co-deposited metal.

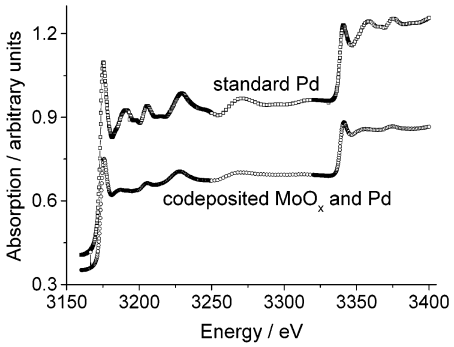

Figure 4. L absorption edge for the standard Pd and of a modified electrode by Mo species and Pd from solution containing 1 mmol·L^{-1} Mo(VI) and 1 mmol·L^{-1} Pd(II).

The electrochemical co-deposition of Pt, Pd, and Rh with molybdenum oxides originates a structure enriched with a mixture of tetrahedral and octahedral Mo sites. The Cu co-deposition changed the film structure to mostly tetrahedral coordinated Mo sites.

The magnitude of the splitting of the L_3 edge doublet is in the range that characterize an octahedral coordination of Mo in films prepared with no metal co-deposition and with Pd or Rh co-deposition from diluted solutions of metallic cations. Tetrahedral and octahedral units of Mo oxides are present in molybdenum oxide films containing Pt or Cu. According to Lede et al.,[47] by employing more concentrated modifier solutions, the enrichment in tetrahedral units also occurs in films obtained with other metals co-deposition, demonstrating that the Mo 4d level should be different even when the Mo coordination is the same for all Mo atoms.

Films containing co-deposited Pd present the L_3 absorption edge at the same energy value as the standard metallic Pd (Figure 4), revealing the formation of metallic particles within the MoO_x structures. The L_3 absorption peaks, observed for the electrochemically grown film, appear at similar energy values as those obtained with standard Pd, even though the absorption intensity is slightly lower. This may be an indication that Pd exists in the films as a material supported in the oxide substrate, retaining its medium range organization in the form of nanoagglomerated structures. The same behavior was observed for films prepared by using working solutions containing 1 mmol·L^{-1} Mo(VI) and 0.1 mmol·L^{-1} Pd(II), but the peak intensities are attenuated. For electrodes modified in solutions 10 times more diluted in Pd(II), no Pd signal was identified as a consequence of the equipment sensitivity and the decrease in the superficial area of the nanoagglomerates. The area under the absorption edge of the co-deposited Pd (3.45) is lower than that of the standard Pd (6.16), corroborating the conclusion that the Pd has some effects on the Mo 4d level; that is, it is possible that a Mo−O−Pd bond takes part in the process of co-deposition.[44]

Differently from Pd, Mo(VI) films with co-deposited Rh do not present medium range organization since the absorption peaks are very attenuated in comparison

(44) Chen, J. G. *Surf. Sci. Rep.* **1997**, *30*, 1.
(45) Kunimori, K.; Wakasugi, T.; Yamakawa, F.; Oyanagi, H.; Nakamura, J.; Uchijima, T. *Catal. Lett.* **1991**, *9* (5−6), 331.
(46) Matsuda, T.; Uchijima, F.; Endo, S.; Takahashi, N. *Appl. Catal., A* **1999**, *176* (1), 91.
(47) Lede, E. J.; Requejo, F. G.; Pawelec, B.; Fierro, J. L. G. *J. Phys. Chem. B* **2002**, *106*, 7824.

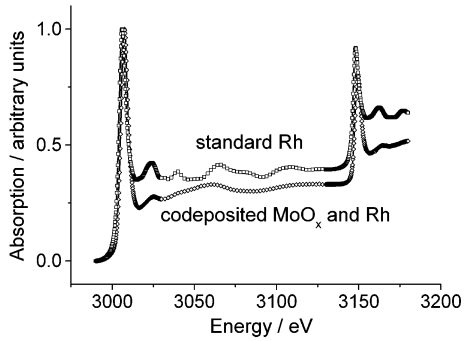

Figure 5. L absorption edge for the standard Rh and of a modified electrode by Mo species and Rh from solution containing 1 mmol·L^{-1} Mo(VI) and 1 mmol·L^{-1} Rh(III).

with standard metallic Rh (Figure 5), even for films prepared by using Mo(VI) and Rh(III) equimolar solutions. The nanoagglomerated structure is preserved in the film; however, it should have lower dimensions and be more dispersed than the Pd particles. Rh signals in the films prepared from solutions containing Rh(III) in concentrations lower than 1 mmol·L^{-1} were not observed. The position of the absorption edge indicates that the deposited Rh is in the metallic state. Also, the relatively small area difference between standard Rh (7.82) and co-deposited Rh (6.82) absorption peak areas suggests that no significant changes occur in the electronic distribution of Rh by the electrochemical co-deposition.

An additional difficulty of Pt analysis by XAS is that the Mo L_2 edge and the Pt M_3 edge are very close. Despite this, because of the good equipment resolution, both edges were satisfactorily separated. Results shown in Figure 6 indicate that there is no medium range organization of Pt particles when this metal is co-deposited with molybdenum oxide. The peaks are weaker than those of standard Pt. This suggests that Pt nanoparticles are more effectively dispersed as small agglomerates in the porous film substrate than the other metals studied. The area under the absorption edge does not change significantly, which suggests that platinum is not chemically bound to molybdenum, in agreement with XRD results reported by Ioroi et al.[4]

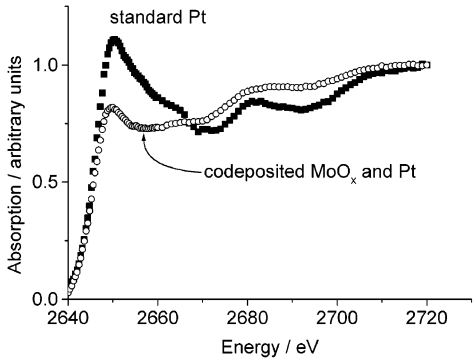

Figure 6. M absorption edge for the standard Rh and of a modified electrode by Mo species and Pt from solution containing 1 mmol·L^{-1} Mo(VI) and 1 mmol·L^{-1} Pt(II).

Conclusions

The thickness of the electrochemically deposited Mo films is proportional to the number of potential cycles used in the modification in Mo(VI)-containing solution. The co-deposition of Pt intensifies the process of deposition of Mo species and Pt and Cu favor the formation of bronzes. All the metal additives modify the Mo oxidation state, reducing it.

The coordination of electrodeposited MoO_x has been established as octahedral units by using XAS at the Mo L_2 and L_3 edges. The co-deposition of Pd and Rh did not change significantly this conformation, but the co-deposition of Pt and Cu enriched the film with tetrahedral structures.

Co-deposited metals are in the metallic state of oxidation and present nanoagglomerated structure with medium range organization. There are indications that Pd co-deposition forms Pd−Mo or Pd−O−Mo bonds.

Acknowledgment. Authors would like to thank FAPESP (Fundação de Amparo à Pesquisa do Estado de São Paulo) and CNPq (Conselho Nacional de Desenvolvimento Científico e Tecnológico) for financial support and LNLS (Laboratório Nacional de Luz Síncrotron) for the use of the SXS line.

CM040125T